Computational Validation of the Scaling Rules for Fluidized Beds

J. Ruud van Ommen[1], Sijbe Sijbesma[1], John Nijenhuis[1], Berend G.M. van Wachem[2]

[1]Delft University of Technology, Reactor & Catalysis Engineering
Julianalaan 136, 2628 BL Delft, the Netherlands; E-mail: j.r.vanommen@tnw.tudelft.nl

[2]Chalmers University of Technology, Department of Thermo and Fluid Dynamics
SE-41296, Göteborg, Sweden; E-mail: berend@tfd.chalmers.se

Introduction

Proper scaling from laboratory-scale to full scale is still *the* major challenge when using fluidized beds for processes in chemical industry. Often, fluidized beds behave differently on the large scale than on lab-scale, which is an obstacle for the testing and development of industrial applications of fluidized bed reactors. One example is that bubbles rise faster in larger fluidized beds, due to decreased wall effects, and have less exchange with the dense phase. When an industrial fluidized bed installation with a novel design is planned, this often requires first studying a pilot-scale model to avoid unexpected effects at the large scale: direct scaling-up from lab-scale to industrial scale is very risky.

Scaling rules based on dimensionless groups have been proposed to facilitate scaling (*e.g.*, Fitzgerald and Crane, 1980, Glicksman, 1984), but they give the problem of contradictory demands or at least experimentally difficult demands (*e.g.*, the need of exotic gases or particles to obtain a certain density and/or viscosity ratio). *Simplified* scaling rules have been proposed to overcome these problems (e.g, Horio *et al.*, 1986, Glicksman, 1988), but it is unsure if the exclusion of certain dimensionless groups deteriorates the scaling quality. The dimensionless groups arise from the strongly simplified Eulerian-Eulerian governing equations for multiphase flow. In validating the simplified scaling rules by performing experiments at various scales, discussion remains if a disagreement is due to failing of the simplified scaling rules or incorrect execution of the experiments.

In the present study, we employ a Eulerian-Eulerian computational fluid dynamics code, employing kinetic theory of granular flow, to model fluidized beds of various sizes to study the difference in behaviour. The goal is to obtain a reliable conclusion on the applicability of the various sets of existing scaling rules. Moreover, the importance of the various dimensionless groups in the scaling rules are studied, which can lead to an improvement of existing scaling rules.

Scaling rules

Full set
Glicksman (1984) obtained the full set of scaling parameters by non-dimensionalisation of the mass and momentum balances along with their boundary conditions. Important assumptions used in deriving the parameters are:

- The fluid is incompressible
- Inter-particle forces other than mechanical forces due to collisions are omitted
- The influence of the particle coefficient of restitution and the friction coefficient on inter-particle collisions is not included

With these assumptions, the following set is derived (Glicksman, 1984):

$$\frac{u_o^2}{gL}, \frac{\rho_s}{\rho_g}, \frac{\beta L}{\rho_s u_o}, \frac{L_1}{L_2}, \frac{G_s}{\rho_s u_o}, \frac{P_o}{\rho_g u_o^2} \qquad (1)$$

G_s expresses the solids circulation rate for circulating fluidized beds and is not relevant for the captive fluidized beds we focus on in this study. It is important that the reactor configuration is equal on both scales. This applies to internals, distributor configuration and bed height-to-width ratio and ratios of other geometrical bed dimensions, and is expressed in the $\frac{L_1}{L_2}$ term. The $\frac{\beta L}{\rho_s u_o}$ term, containing the fluid-to-particle drag coefficient, is related to the Ergun equation (low gas velocities, dense bed) or to the expression for single sphere drag (high gas velocities, diluted bed). When the Ergun equation is non-dimensionalised it is shown that this term depends on the Reynolds number and $\frac{L}{d_p}$. By substituting these equations into Eq. (1), the following set of dimensionless parameters emerges, which is called the full set:

$$\frac{u_o^2}{gL}, \frac{\rho_s}{\rho_g}, \frac{\rho_g u_o d_p}{\mu}, \frac{L}{d_p}, \frac{L_1}{L_2}, \phi, \textit{particle size distribution} \qquad (2)$$

The particle size distribution and the sphericity of the particles should be equal. Glicksman (1984) assumed that the $\frac{P_o}{\rho_s u_o^2}$ group could be neglected in the case of low gas velocities relative to the speed of sound. This assumption provides a degree of freedom in scaling simulated fluidized beds. This group would fix ρ_s in scale-up. By neglecting this group, values of ρ_s, μ and ρ_f can be varied while keeping the Reynolds numbers constant. Glicksman also omitted the particle and gas stress tensors and the pressure gradient term in the derivation of the scaling rules. The equation expressing this last term was non-dimensionalized by Foscolo *et al.* (1990) and yielded the Froude number, which was already included in the set.

Simplified set

In practice, it is found to be difficult to match all parameters expressed in the full set of scaling parameters. To be able to match these parameters, it will often be needed to use very exotic particles and gases. To overcome this problem, Glicksman *et al.* (1993) derived the simplified set, which includes less parameters than the full set. The drag coefficient is expressed in a simplified form of the Ergun equation for different regimes. The set given in Eq. (3) was derived at low and high Reynolds numbers.

$$\frac{u_o^2}{gL}, \frac{\rho_s}{\rho_g}, \frac{u_o}{u_{mf}}, \frac{L_1}{L_2}, \phi, \textit{particle size distribution} \qquad (3)$$

Also for this set all geometrical properties should be equal for both beds. Glicksman *et al*. (1993) assume that it is reasonable to expect that this set is valid over the entire range of conditions for which the Ergun equation holds.

Viscous limit set

The viscous limit set was derived by Glicksman (1988) for dense fluidized beds, at low gas velocities, with $\frac{\rho_g u_o d_p}{\eta} < 4$. In this region the viscous forces are dominant over the inertia forces. Due to the negligible inertia forces the requirements for scaling are less stringent. The Ergun equation is limited to its first term, which expresses the drag resulting from viscous forces. The $\frac{\beta L}{\rho_s u_o}$ term in this case is proportional to $\frac{u_o^2}{gL}$ and $\frac{u_o}{u_{mf}}$. This results in a lower number of dimensionless parameters that have to be matched for correct scaling:

$$\frac{u_o^2}{gL}, \frac{u_o}{u_{mf}}, \frac{L_1}{L_2}, \phi, \textit{particle size distribution} \qquad (4)$$

Simulations

Computational fluid dynamics (CFD) is a method used for design and optimisation in a wide range of engineering applications such as aircraft, pumps, and other equipment related to single phase operations. CFD models are seldom applied to gas-solid flow in industry. The models that are used nowadays can be divided in two groups, Eulerian-Lagrangian models and Eulerian-Eulerian models. Eulerian-Lagrangian models calculate and describe the path of discrete particles in the gas flow. This type of modelling requires a large amount of memory and long calculation times. In this paper the Eulerian-Eulerian approach is used. This approach describes the particle phase as a continuum and averages out the single particle properties. The advantage of Eulerian-Eulerian modelling is that less memory and computational time is necessary. To be able to describe the particles as a continuum the kinetic theory of granular flow, which is derived from the kinetic theory of gasses, is used. The two phases are considered to be continuous and fully interpenetrating. Computations with this model can predict the behaviour of dense-phase particle flows on a realistic geometry. For details on kinetic theory of granular flow see van Wachem *et al.* (2001).

The simulations are performed with the aid of CFX 4.4. The source code of the two-fluid model based on kinetic theory for granular flow was implemented and validated by van Wachem *et al.* (2001). For details on used discretisation algorithms, pressure correction equations and simulation boundary conditions see van Wachem *et al.*. The coefficient of restitution, expressing elasticity in collisions between particles was set to 0.9. Initial bed voidage was set to 0.36 based on random packing of spheres. The simulations are limited to two two-dimensional geometries in which front and back wall effects are neglected. The used rectangular computational grids for the reference and scaled fluidized bed consist of square cells of a height and width of 1 cm x 1 cm and 0.5 cm x 0.5 cm respectively. The grid spacing was scaled to obtain the same resolution in the simulations in different scales to be able to compare data from the same dimensionless location.

The grid spacing of 1 cm x 1 cm was determined by van Wachem *et al.* (2001), by changing the size until average properties changed by less than 4%. Time discretisation was done with

fixed time stepping of $1 \cdot 10^{-4}$ s. If simulations did not converge, the fixed time step was set to $0.7 \cdot 10^{-4}$ s or $0.6 \cdot 10^{-4}$ s. Pressure and voidage values for every grid point were written to a binary data file at 1000 Hz. At start up of the simulations the time stepping was stepwise changed from $0.5 \cdot 10^{-4}$ to $1 \cdot 10^{-4}$ s. Also a jet disturbance is used for 1 s of real time to break bed symmetry, which leads to faster stationary fluidization of the bed. To obtain reasonable data sets to compare the large and scaled bed, 49 and 39 s of real time data was simulated respectively. To avoid the influence of start-up effects, the first 12 s of each simulation was discarded in the signal analysis.

The geometry of the simulated beds was limited to two 2D bed geometries that are scaled with a scaling factor m = 2. Details are shown in Table 1. These geometries where chosen to limit the necessary computational time to obtain a reasonably large time series of pressure and voidage data The mesh size was 1 x 1 cm for the large bed and 0.5 x 0.5 cm for the small bed.

Table 1 Bed geometries used in the simulations

	Large bed	**Small bed**
Domain height [m]	0.60	0.30
Width [m]	0.30	0.15
Settled bed height [m]	0.20	0.10

As reference three large bed simulations were carried out at three different particle Reynolds numbers. For every large reference bed three small beds were scaled according to the full, simplified and viscous limit set. The particle and gas properties used in these simulations and the used gas velocities are shown in Table 2.

Table 2 Parameter settings for the reference bed (large scale) and the small beds scaled using the full, simplified and viscous limit set.

Set	d_p [μm]	ρ_s [kg/m^3]	ρ_g [kg/m^3]	η_g [Pa·s]	u_o [m/s]	u_{mf} [m/s]	Re_p [-]
Reference	396	2600	1.205	$1.82 \cdot 10^{-5}$	0.566	0.126	14.83
Full	198	2012	0.932	$4.98 \cdot 10^{-6}$	0.400	0.089	14.83
Simplified	329	2600	1.205	$1.82 \cdot 10^{-5}$	0.400	0.089	8.73
Viscous limit	469	1300	1.205	$1.82 \cdot 10^{-5}$	0.400	0.089	12.43
Reference	361	2600	1.205	$1.82 \cdot 10^{-5}$	0.3577	0.1065	8.55
Full	181	2012	0.932	$4.98 \cdot 10^{-6}$	0.2530	0.0752	8.55
Simplified	301	2600	1.205	$1.82 \cdot 10^{-5}$	0.2530	0.0752	5.05
Viscous limit	428	1300	1.205	$1.82 \cdot 10^{-5}$	0.2530	0.0752	7.17
Reference	264	2600	1.205	$1.82 \cdot 10^{-5}$	0.130	0.0581	2.27
Full	132	2012	0.932	$4.98 \cdot 10^{-6}$	0.092	0.0411	2.27
Simplified	221	2600	1.205	$1.82 \cdot 10^{-5}$	0.092	0.0411	1.35
Viscous limit	313	1300	1.205	$1.82 \cdot 10^{-5}$	0.092	0.0411	1.91
Re_p *is defined as* $\frac{\rho_g u_o d_p}{\eta}$							

The advantage of simulations is that time-series of physical properties can easily be obtained at arbitrary positions in the bed without disturbing the hydrodynamics. Moreover, it is easier to exactly match the criteria dictated by the scaling rules. For example, finding particles with a

given density can be hard in practice, but in simulations the density value can easily be adapted. A disadvantage of the simulations is the long calculation times that are needed. It would be preferably to have time-series in the order of several minutes for the signals analysis. While this criterion is already often not met in experimental papers on scale-up, it would require excessive calculation times in the computational validation of the scaling rules. We will use time-series of 37 s for the large scale and 27 s for the small scale.

Signal analysis

In this paper, we will use pressure and voidage signals to investigate the correctness of the scaling. Pressure signals have often been used in experimental studies of scaling fluidized beds, since pressure is easy to measure and gives a characterization of the global hydrodynamics. Voidage signals give an indication of the bubble behaviour only at the measurement position in the bed. Both signals are obtained at 16 positions in the bed: the vertical position is 0, 25, 50 en 75% of the settled bed height (denoted as h = 0, 0.25, 0.50, 0.75) and the radial position is at the left wall, halfway the left wall and the centre, in the centre, and halfway the centre and the right wall (denoted as r = 1, 0.50, 0, -0.50).

In the past, the validation of scaling rules has often been carried out using qualitative analysis methods: plots such as probability density functions or power spectra are visually compared. One step to drawing firmer conclusions would be to carry out the analysis in a more quantitative way, for example using statistical tests that judge whether or not a difference is significant. We will use the Kolmogorov Smirnov test applied to the cycle time distribution and the attractor comparison test applied to attractors.

Comparing cycle time distributions

The Kolmogorov Smirnov test is a standard statistical test to judge whether or not two probability density functions show a significant difference. The test yields a *P*-value (probability value). *P*>0.05 indicates that the null hypothesis that the two distributions are similar is not rejected. We apply this test to the cycle time distribution: the probability density function of the cycle times of the signal. Figure 1 shows how the cycle time is determined from the pressure signal. Although the cycle time distribution is focussing on the macro-scale, it is a more sensitive tool for judging differences in time-scales in fluidized bed signals than the power spectral density (van Ommen et al, 1999). We will investigate the cycle time distribution both for the pressure and the voidage signal.

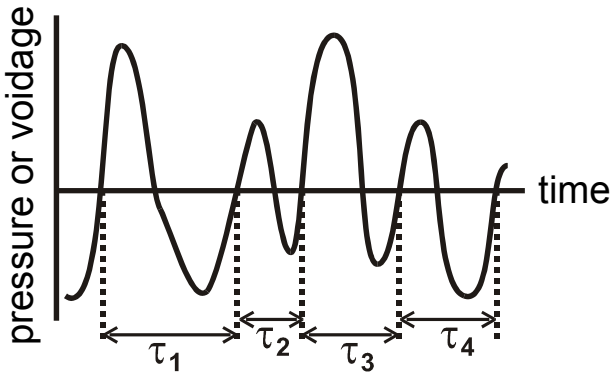

Figure 1 Determination of the cycle times τ_i from a pressure fluctuation signal.

Comparing attractors

A more complete, but less conventional way of judging the similarity in signals is the attractor comparison method. We have shown that the attractor comparison method is a sensitive tool

that can be used for the early detection of agglomeration (Van Ommen *et al.*, 2000, Korbee *et al.*, 2003) and for judging the similarity obtained in scaling fluidized beds (Van Ommen *et al.*, 2004). The attractor comparison method is based on the transformation of a signal into an attractor: a multi-dimensional distribution in the state space. Subsequently, two attractors are compared using a statistical test. An attractor is a multi-dimensional distribution of delay vectors containing successive pressure values (see Figure 2a). The attractor represents consecutive states of the dynamic system: it can be seen as a 'fingerprint' of the fluidized bed hydrodynamics as reflected by the pressure fluctuations in the bed. The attractors obtained at the two scales are compared by calculating a statistic *S* using the Diks *et al.* (1996) test (see Figure 2b). For a more detailed description of the procedure, the reader is referred to Van Ommen *et al.* (2000). *S* represents the dimensionless distance between the two attractors. In this way all attractor properties are taken into account. For attractors generated by the same dynamics or mechanism, *S* has an expectation value of zero and a standard deviation of unity. When *S* is larger than three, we know with more than 95% confidence that the two attractors differ significantly, which means that the hydrodynamic behaviour of the fluidized beds differs. The attractor comparison method is also applied to both pressure and voidage signals.

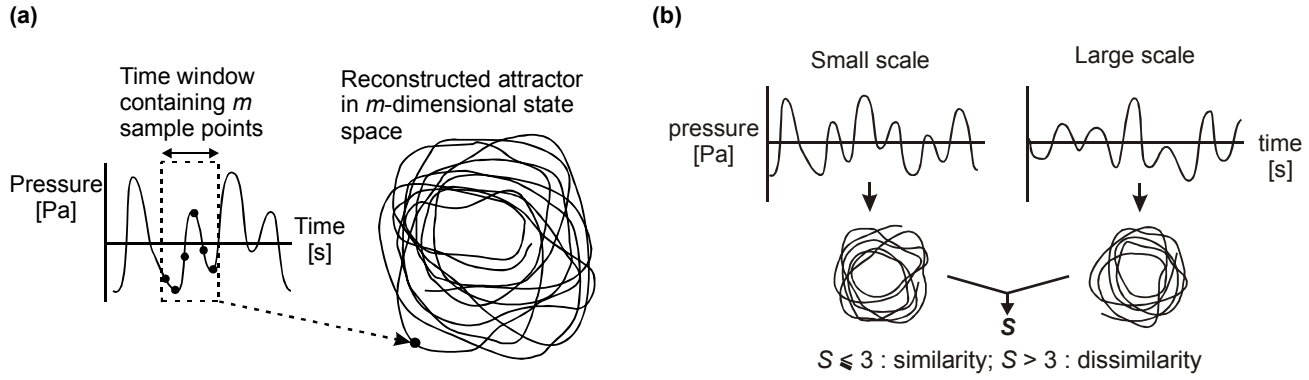

Figure 2. Schematic representation of (a) the reconstruction of an attractor from a pressure fluctuation signal, and (b) the comparison of attractors from different scales by the attractor comparison.

Results and discussion

Cycle time distributions are obtained from pressure and voidage data for the large bed and the three scaled small beds. The distributions are compared with the Kolmogorov-Smirnov test. If the test yields a *P*-values below 0.05, then the two scales show a significant difference in the signals (indicated with grey in the tables). Table 3 gives the results for comparing the cycle time distributions derived from the pressure signals. The table shows that the largest discrepancies are obtained for the low particle Reynolds number. For both the intermediate and high Reynolds number, the simplified set leads to a reasonable good scaling: for 13 of the 16 positions no significant differences are found. Table 4 compares the cycle time distributions for the voidage signal. It shows similar trends as for the pressure signal, but on the whole more significant differences are found for the comparison of the voidage signals.

Table 3 *P*-values obtained from the Kolmogorov Smirnov test applied to cycle time distributions for the pressure signals from large and scaled small beds. Significant differences are indicated with grey. *h* indicates the axial position; *r* indicates the radial position in the bed.

	Full set				**Simplified set**				**Viscous limit set**			
High Re_p												
0.75	0.05	0.00	0.00	0.01	0.09	0.06	0.01	0.04	0.28	0.74	0.23	0.00
0.50	0.00	0.00	0.00	0.00	0.08	0.049	0.08	0.58	0.09	0.09	0.43	0.03
0.25	0.00	0.00	0.02	0.15	0.09	0.49	0.49	0.47	0.02	0.45	0.99	0.55
0.00	0.00	0.00	0.00	0.02	0.00	0.13	0.53	0.67	0.00	0.37	0.36	0.66
Intermediate Re_p												
0.75	0.70	0.22	0.00	0.23	0.00	0.04	0.27	0.53	0.00	0.58	0.02	0.31
0.50	0.72	0.12	0.00	0.04	0.12	0.63	1.00	0.90	0.00	0.01	0.29	0.34
0.25	0.45	0.62	0.02	0.13	0.36	0.01	0.43	0.01	0.00	0.00	0.93	0.04
0.00	0.00	0.00	0.00	0.00	0.75	0.35	0.48	0.33	0.00	0.53	0.00	0.02
Low Re_p												
0.75	0.00	0.00	0.00	0.00	0.01	0.00	0.00	0.00	0.45	0.00	0.00	0.00
0.50	0.00	0.00	0.00	0.00	0.00	0.00	0.00	0.00	0.00	0.00	0.15	0.00
0.25	0.01	0.00	0.00	0.00	0.00	0.09	0.03	0.01	0.00	0.49	0.02	0.03
0.00	0.00	0.00	0.00	0.00	0.00	0.00	0.00	0.00	0.00	0.20	0.00	0.01
h↑ r →	**1.00**	**0.50**	**0.00**	**-0.50**	**1.00**	**0.50**	**0.00**	**-0.50**	**1.00**	**0.50**	**0.00**	**-0.50**

Table 4 *P*-values obtained from the Kolmogorov Smirnov test applied to cycle time distributions for the voidage signals from large and scaled small beds. Significant differences are indicated with grey. *h* indicates the axial position; *r* indicates the radial position in the bed.

	Full set				**Simplified set**				**Viscous limit set**			
High Re_p												
0.75	0.63	0.08	0.00	0.11	0.92	0.67	0.03	0.33	0.24	0.01	0.13	0.00
0.50	1.00	0.02	0.00	0.16	0.61	0.94	0.77	0.98	0.05	0.00	001	0.00
0.25	0.06	0.03	0.00	0.02	0.64	0.14	0.15	0.57	0.01	0.00	0.04	0.00
0.00	0.01	0.00	0.00	0.00	0.53	0.01	0.00	0.00	0.00	0.00	0.00	0.00
Intermediate Re_p												
0.75	0.68	0.01	0.07	0.13	0.75	0.01	0.00	0.42	0.00	0.00	0.00	0.01
0.50	0.01	0.11	0.00	0.60	0.52	0.29	0.01	0.21	0.00	0.01	0.00	0.00
0.25	0.07	0.00	0.00	0.35	0.44	0.00	0.00	0.00	0.00	0.16	0.00	0.00
0.00	0.11	0.00	0.00	0.18	0.06	0.00	0.00	0.00	0.00	0.02	0.00	0.00
Low Re_p												
0.75	0.00	0.00	0.02	0.00	0.00	0.00	0.06	0.00	0.00	0.00	0.00	0.00
0.50	0.00	0.00	0.00	0.00	0.00	0.00	0.01	0.00	0.00	0.00	0.00	0.00
0.25	0.00	0.00	0.00	0.00	0.00	0.00	0.00	0.00	0.00	0.02	0.00	0.88
0.00	0.00	0.00	0.00	0.00	0.00	0.00	0.00	0.00	0.00	0.00	0.00	0.16
h↑ r →	**1.00**	**0.50**	**0.00**	**-0.50**	**1.00**	**0.50**	**0.00**	**-0.50**	**1.00**	**0.50**	**0.00**	**-0.50**

The *S*-values from attractor comparison of pressure signals are given in Table 5; Table 6 gives the same for the voidage signals. Both tables show trends that are very comparable with those for the cycle time distribution: better results for higher particle Reynolds numbers and for the simplified set. Using attractor comparison, the pressure signals yield less significant differences than the voidage signals. We do not yet have an explanation for the difference from the cycle time distribution analysis. At intermediate and high Reynolds numbers, the attractor comparison method applied to the pressure signal indicates no significant differences when the scaling is carried out using the simplified set.

Table 5 *S*-values obtained from attractor comparison applied to the pressure signals from large and scaled small beds. Significant differences are indicated with grey. *h* indicates the axial position; *r* indicates the radial position in the bed.

	Full set				**Simplified set**				**Viscous limit set**			
High Re_p												
0.75	0.5	1.9	4.6	0.1	-0.6	1.8	-0.4	-0.1	-0.9	-0.2	1.6	3.0
0.50	1.8	4.1	5.5	-0.6	1.0	-0.5	-0.3	-1.5	1.38	0.5	1.9	-0.4
0.25	3.0	3.6	3.3	1.0	0.5	0.5	-0.8	0.1	1.85	4.2	0.9	0.9
0.00	4.8	2.8	1.7	0.1	0.6	-0.2	-1.1	-0.5	1.23	0.4	-0.1	2.4
Intermediate Re_p												
0.75	1.4	-0.2	1.6	-0.3	-0.3	-0.5	-1.1	-0.7	2.6	4.1	0.9	-1.5
0.50	-0.9	4.0	4.2	1.2	-0.1	0.0	-0.5	-1.6	4.1	0.7	1.0	-1.2
0.25	0.6	1.6	2.9	2.3	1.8	2.6	-1.1	0.1	3.4	0.8	0.4	0.0
0.00	2.4	1.0	2.7	1.5	1.6	-1.1	-0.6	-0.9	1.5	-1.0	0.2	0.7
Low Re_p												
0.75	4.0	0.2	1.3	0.9	1.8	1.6	1.6	3.4	-0.7	0.2	5.3	-0.1
0.50	6.8	3.6	4.1	2.0	1.1	1.7	0.4	2.4	0.5	1.5	7.2	0.1
0.25	6.3	12.6	5.4	10.3	2.2	4.6	0.9	4.3	0.2	5.5	5.0	2.3
0.00	11.9	9.0	5.5	9.3	0.2	2.4	0.2	1.0	1.1	2.4	4.5	2.7
h↑ r →	**1.00**	**0.50**	**0.00**	**-0.50**	**1.00**	**0.50**	**0.00**	**-0.50**	**1.00**	**0.50**	**0.00**	**-0.50**

Table 6 *S*-values obtained from attractor comparison applied to the voidage signals from large and scaled small beds. Significant differences are indicated with grey. *h* indicates the axial position; *r* indicates the radial position in the bed.

	Full set				**Simplified set**				**Viscous limit set**			
High Re_p												
0.75	14.0	3.3	10.9	13.5	4.1	1.6	2.8	1.1	3.9	1.1	18.3	29.5
0.50	8.4	4.1	6.0	8.1	0.1	-0.4	1.2	-0.2	13.5	3.6	28.1	25.0
0.25	2.8	3.3	1.5	16.9	0.2	3.4	1.4	1.0	7.5	4.7	8.8	2.4
0.00	0.1	3.4	3.0	0.5	-0.5	-0.2	0.0	2.5	2.4	6.6	0.1	9.8
Intermediate Re_p												
0.75	16.0	0.1	2.9	24.1	2.5	22.2	4.7	2.8	40.7	11.6	9.0	1.3
0.50	7.4	2.1	6.0	13.7	1.4	8.3	3.9	6.1	31.6	15.4	5.9	9.7
0.25	0.9	3.4	8.9	15.5	1.5	13.9	-0.7	7.5	21.3	11.2	7.2	7.1
0.00	-0.6	-0.1	2.1	5.0	2.3	1.6	0.7	8.7	6.7	7.4	0.3	10.5
Low Re_p												
0.75	24.0	13.0	31.9	13.9	13.4	6.0	23.8	5.3	12.6	1.6	19.2	-0.2
0.50	20.5	14.7	22.8	11.7	19.0	8.2	19.0	4.1	16.3	1.9	14.7	0.8
0.25	16.8	9.2	17.4	4.0	10.8	3.2	7.1	2.8	8.0	0.3	12.6	-0.6
0.00	11.3	14.5	8.3	11.3	8.6	6.1	1.7	7.7	1.5	6.2	1.8	1.3
h↑ r →	**1.00**	**0.50**	**0.00**	**-0.50**	**1.00**	**0.50**	**0.00**	**-0.50**	**1.00**	**0.50**	**0.00**	**-0.50**

The results show that in general the agreement is best for the simplified set. It is surprising that the full set – which is stricter than the simplified set – leads to worse results. An explanation could be that one or more groups that are not included in the full set are implicitly kept constant or are changed less because of our choice of variables for the simplified set. For example, the group $\frac{P_o}{\rho_s u_o^2}$, that Glicksman (1984) ignores even in the full set, changes with a factor 2.6 for the full set simulations and with a factor 2.0 for the simplified set simulations. At the moment, no firm conclusions can yet be drawn; we are carrying out simulations with other choices of operating conditions to investigate this point.

The attractor comparison analysis of the pressure signals leads to more positive results about the correctness of the scaling than the analysis of the voidage signals; the cycle time distributions do not display much difference between pressure and voidage signals. In general, the attractor comparison method applied to relatively short time-series will be more reliable, since it uses all available data points, while the determination of the cycle times yields only a few values per second (*i.e.*, each second of the signal contains a few cycles). However, for both techniques more firm conclusions could be drawn if the simulations were run for some minutes instead of the time-series of about half a minute used in this paper. We are currently working on this.

The simulated bed movies show that for the low particle Reynolds numbers bubbles just start to form in the upper regions of the bed, and that the emulsion phase in the lower part seems to be instable and only periodically shows bubble formation and voidage waves. This may indicate that the bed is oscillating between two states and thus is not stationary. This may be an explanation for the large deviations at the low Reynolds numbers. Probably, longer time-series are most important at these low gas velocities.

Sanderson (2003) found from experiments that the similitude between scales improved when moving towards the centre of the bed and when moving downward in the bed. In our simulations, the extent of similitude does not seem to depend on the position in the bed.

Concluding remarks

We compared fluidized beds with a size difference of a factor two using three sets of scaling rules: the full, the simplified, and the viscous limit set. The comparison was carried out using statistical tests that yield a quantitative measure whether or not similitude between the scales was obtained. These tests are applied to pressure and voidage signals obtained at 16 positions in the bed. The testing of the various positions does not yield an unambiguous result.

We found that the simplified set yields the best results, which is surprising since this set of scaling rules is less stringent than the full set. Possibly, we implicitly obeyed certain rules that are included in none of the three sets when choosing the operating conditions for the simplified set simulations. We further found that largest differences are obtained for low particle Reynolds numbers.

We are continuing this study in order to reach firmer conclusions. By varying different operating conditions, we investigate why the simplified set performs so well in comparison with the full set. Moreover, longer simulation runs will be carried out in order to achieve a more reliable time-series analysis.

References

Diks, C., van Zwet, W.R., Takens, F., DeGoede, J., Detecting differences between delay vector distributions, *Physical Review E*, **53,** 2169-2176, 1996.

Fitzgerald, T.J., Crane, S.D., Cold fluidized bed modeling, *Proceedings of 6th International Conference on Fluidized Bed Combustion*, Atlanta, 815-820, 1980.

Foscolo, P. U., Di Felice, R., Gibilaro, L. G., Pistone, L., Piccolo, V., Scaling relationships for fluidisation: the generalised particle bed model, *Chemical Engineering Science*, **45**, 1647-1651, 1990.

Glicksman, L. R., Scaling relationships for fluidised beds, *Chemical Engineering Science*, **39,** 1373-1379, 1984.

Glicksman, L. R., Scaling relationships for fluidised beds, *Chemical Engineering Science*, **43,** 1419-1421, 1988.

Glicksman, L. R., Hyre, M. and Woloshun, K., Simplified scaling relationships for fluidised beds, *Powder Technology*, **77**, 177-199, 1993.

Horio, M., Nonaka, A., Sawa, Y. and Muchi, I., A new similarity rule for fluidised bed scale-up, *AIChE Journal*, **32**, 1466-1482, 1986.

Korbee, R., van Ommen, J.R., Lensselink, J., Nijenhuis, J., Kiel, J.H.A., van den Bleek, C.M., 'Early Agglomeration Recognition System (EARS)', in: *Proceedings of the 17th International Conference on Fluidized Bed Combustion*, ASME, New York, USA, paper 151, 2003.

Sanderson, J. P., *Experimental verification of the simplified scaling laws for bubbling fluidised beds at large scales*, PhD thesis, Monash University, Adelaide, Australia, 2003.

van Ommen, J.R., Schouten, J.C., van den Bleek, C.M., 'An early-warning-method for detecting bed agglomeration in fluidized bed combustors', *Proceedings of the 15th International Conference on Fluidized Bed Combustion*, Reuther, R.B. (Ed.), ASME, New York, USA, paper 150, 1999.

van Ommen, J.R., Coppens, M.-O., van den Bleek, C.M., Schouten, J.C., 'Early warning of agglomeration in fluidized beds by attractor comparison', *AIChE Journal* **46,** 2183-2197, 2000.

van Ommen, J.R., Sanderson, J., Nijenhuis, J., Rhodes, M.J., van den Bleek, C.M, 'Reliable validation of the simplified scaling rules for fluidized beds', in: Arena, U., Chirone, R., Miccio, M. Salatino, P. (Eds.), *Proceedings of the Eleventh Engineering Foundation Conference on Fluidization*, Engineering Conferences International, New York, USA, 451-458, 2004.

van Wachem, B.G.M, Schouten, J.C., Krishna, R., van den Bleek, C.M., Sinclair, J.L., 'Comparative Analysis of CFD Models of Dense Gas-Solid Systems', *AIChE J.* **46**, 1035-1051, 2001.